iScience, Volume *25*

Supplemental information

The role of Phe150 in human voltage-gated proton channel

Xin Wu, Lu Zhang, and Liang Hong

SUPPLEMENTARY INFORMATION

The role of Phe150 in human voltage-gated proton channel

Xin Wu, Lu Zhang, Liang Hong

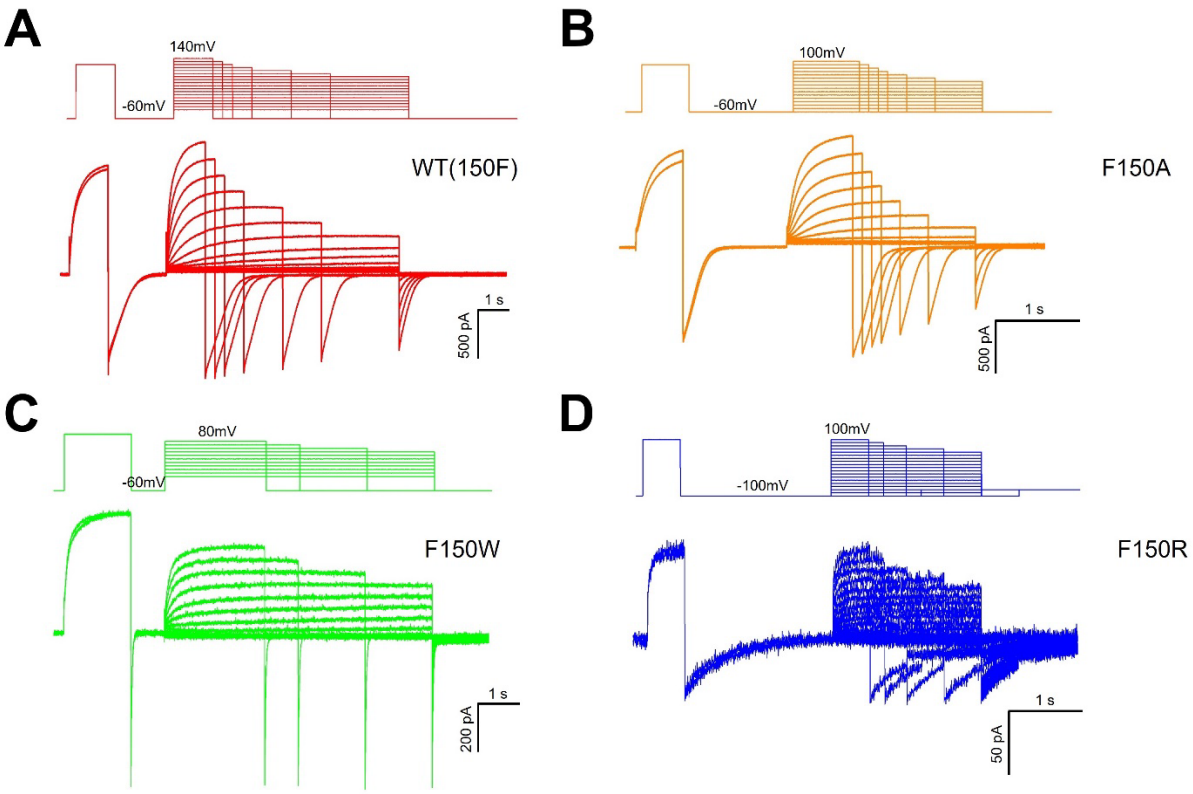

Figure.S1 hH_v1 F150 mutations affect voltage-dependent activation of the channel. Related to Figure 1. Representative currents were recorded in HEK293 cells expressing WT(150F) (**A**), F150A (**B**), F150W (**C**), or F150R (**D**), pH_i=pH_o=6.0. For clarity, only the first and last traces elicited by the depolarization pre-step are shown. The corresponding pulse protocols are shown above the current traces.

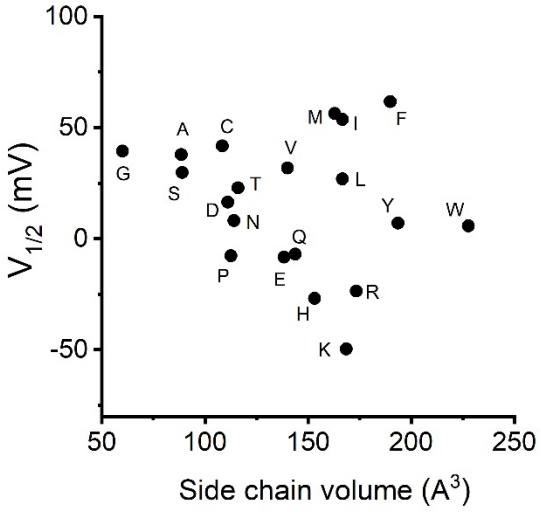

Figure.S2 The size of side chain does not correlate with H_v1 voltage-dependent activation. Related to Figure 1. The $V_{1/2}$ values obtained from *G-V* curves are plotted with size of the substituted side chain at position F150. There were no significant correlations between the size of side chain and the $V_{1/2}$ values.

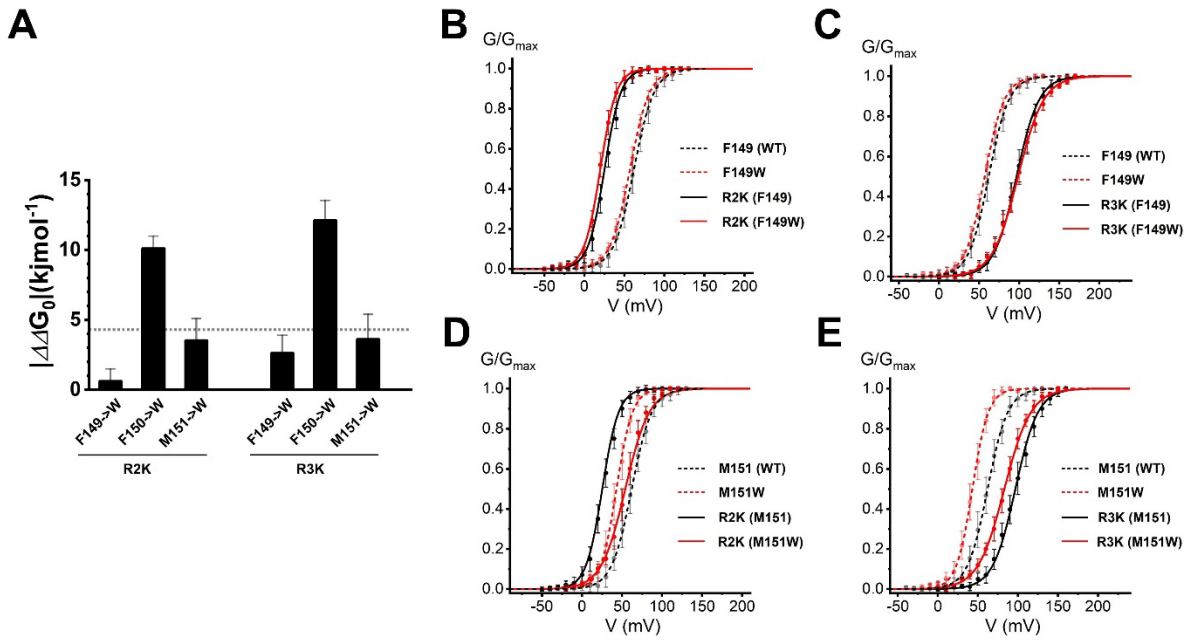

Figure. S3 F149 and M151 do not interact with R2 and R3 during the channel activation. Related to Figure 2. **A.** Summary of $|\Delta\Delta G_0|$ determined by the double mutant cycle analysis. A significant interaction between two residues was defined as a $|\Delta\Delta G_0|$ > 4.2 kJ/mol (dot line). **B-E.** Effects of mutations on the *G-V* relationship of the channels. Voltage-dependent channel activations were shown for R2K with F149 (R2K(F149)) and R2K with F149W (R2K(F149W)) (**B**), R3K(F149) and R3K(F149W) (**C**), R2K(M151) and R2K(M151W) (**E**), and R3K(M151) and R3K(M151W) (**F**). In **B-C**, the dash line (black) represented *G-V* curve of WT channel (F149), and the dash line (red) represented *G-V* curve of F149W. In **D-E**, the dash line (black) represented *G-V* curve of WT channel (M151), and the dash line (red) represented *G-V* curve of M151W. Lines indicate fits of the data to a *Boltzmann* function. Proton currents were recorded in HEK293 cells expressing H_v1 mutations, pH_i=pH_o=6.0. Data are represented as mean ± SEM.

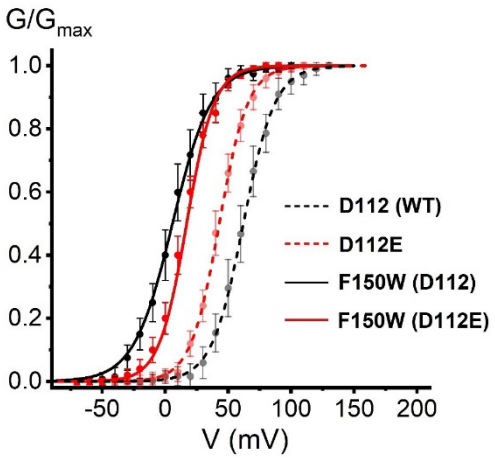

Figure. S4 Double mutant cycle analysis indicates F150 interacts with D112E. Related to Figure 2. Voltage-dependent channel activations were shown for F150W with D112 (F150W(D112)) and F150W with D112E (F150W (D112E)), the dash line (black) represented *G-V* curve of WT channel (D112), and the dash line (red) represented *G-V* curve of D112E. The combination F150W-D112E had $|\Delta\Delta G_0|$ value (6.0 kJ/mol) larger than 4.2 kJ/mol, indicating a thermodynamic coupling between F150 and D112. Lines indicate fits of the data to a *Boltzmann* function. Proton currents were recorded in HEK293 cells expressing H_v1 mutations, pH_i=pH_o=6.0. Data are represented as mean ± SEM.

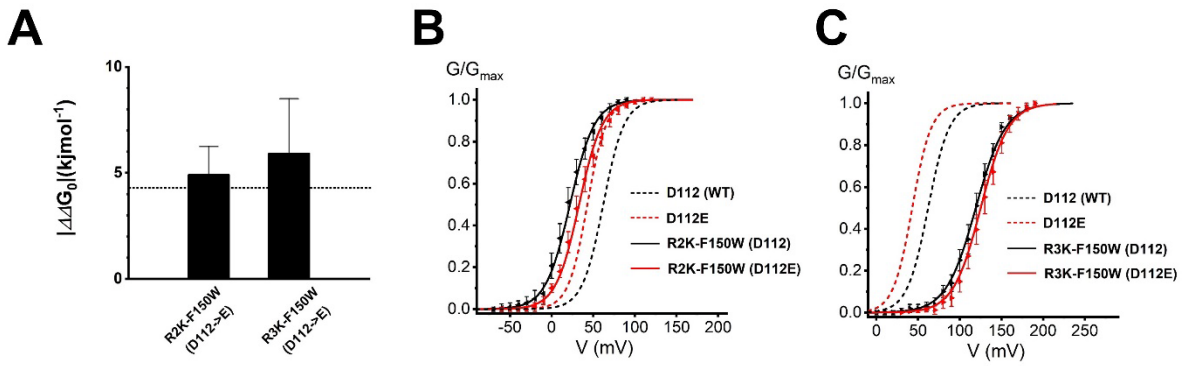

Figure.S5 Effects of D112E on the interactions between F150 and R2/R3. Related to Figure 2. **A.** Summary of $|\Delta\Delta G_0|$ determined by the double mutant cycle analysis. A significant interaction between two residues was defined as a $|\Delta\Delta G_0|$ > 4.2 kJ/mol (dot line). **B-C.** Voltage-dependent channel activations were shown for R2K-F150W with D112 (R2K-F150W(D112)) and R2K-F150W with D112E (R2K-F150W (D112E)) (**B**), R3K-F150W with D112 (R3K-F150W(D112)) and R3K-F150W with D112E (R3K-F150W (D112E)) (**C**). In **B-C**, the dash line (black) represented *G-V* curve of WT channel (D112), and the dash line (red) represented *G-V* curve of D112E. Lines indicate fits of the data to a *Boltzmann* function. Proton currents were recorded in HEK293 cells expressing H_V1 mutations, pH_i=pH_o=6.0. Data are represented as mean ± SEM.

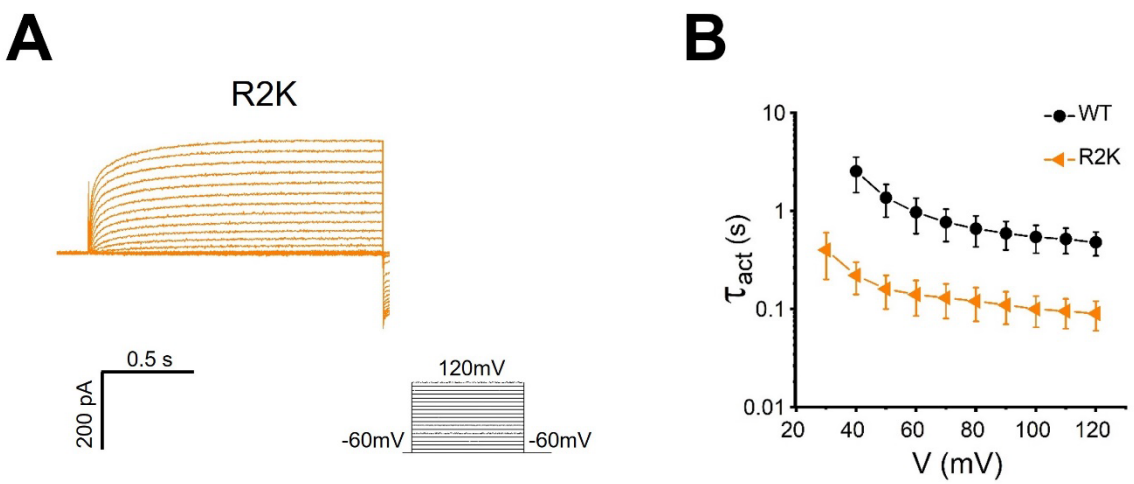

Figure.S6 Effects of R2K on the activation kinetics of the channel. Related to Figure 3. **A.** Representative rising currents recorded from R2K. Currents were measured from a holding potential of -60 mV to test potentials ranging between -60 and +120 mV in 10 mV steps. **B.** The channel opening time constant τ_{act} in WT or R2K mutation. τ_{act} was obtained from *exponential* fit to rising currents. Proton currents were recorded in HEK293 cells expressing H_V1 mutations, $pH_i=pH_o=6.0$. Data are represented as mean ± SEM.

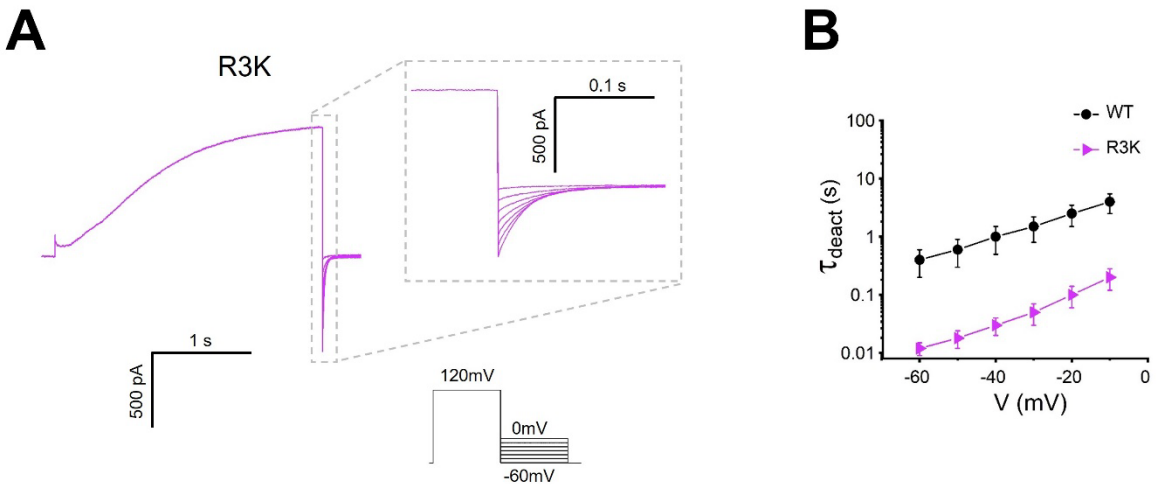

Figure.S7 Effects of R3K on the deactivation kinetics of the channel. Related to Figure 4. **A.** Representative tail currents recorded from R3K. The tail currents were elicited by a prepulse to 120 mV, in 10 mV decrements from 0 to -60 mV. The dotted line box represents the zoomed area. **B.** The deactivation (channel closing) time constant τ_{deact} in WT or R3K mutation. τ_{deact} was obtained from *exponential* fit to tail currents. Proton currents were recorded in HEK293 cells expressing H_v1 mutations, $pH_i=pH_o=6.0$. Data are represented as mean ± SEM.

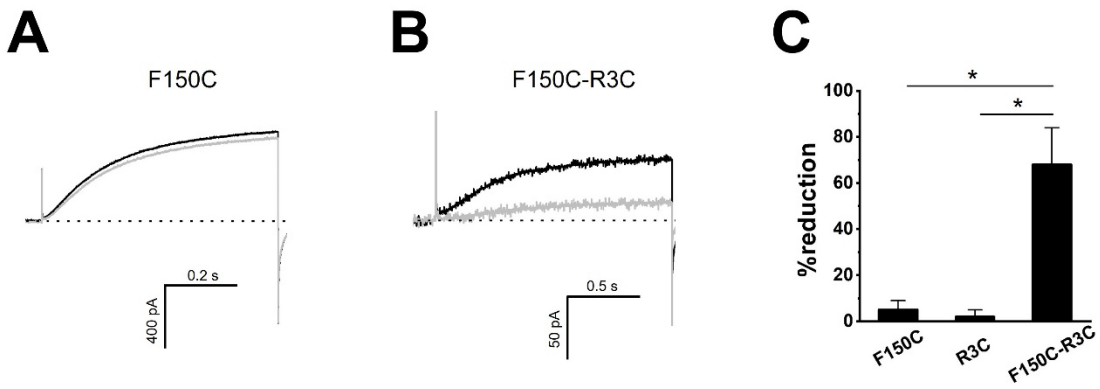

Figure.S8 Cysteine cross linking analysis for positions F150 and R3. Related to Figure 4. **A-B.** Representative proton currents measured in an inside-out patch from a *Xenopus* oocyte expressing H_v1 F150C (**A**) or F150C-R3C (**B**) before (black traces) and after (gray traces) addition 2 μM Cd^{2+} in the bath solution, pH_i=pH_o=6.0. Currents were measured from a holding potential of -60 mV to the test potential of +120 mV in inside-out patch configuration. The dash lines represent 0 pA. **C.** Summary of reduction of proton current produced by Cd^{2+}. Data are represented as mean ± SEM. *p < 0.05, paired, two-tailed Student's t test.

Table.S1 Effects of F150 mutations on the voltage-dependent activation of H_V1 channels. Related to Figure 1.

Channel	*n*	$V_{1/2}$*(mV)*	*k(mV)*
F150A	6	37.9±3.5	10.9±0.6
F150C	8	41.8±3.6	12.1±0.7
F150D	5	16.4±5.1	14.0±0.7
F150E	6	-8.3±3.5	14.5±0.8
150F(WT)	10	61.7±2.7	11.6±0.4
F150G	8	39.4±3.1	13.6±0.7
F150H	8	-26.9±3.4	10.7±0.5
F150I	6	53.7±3.3	11.9±0.6
F150K	5	-49.7±4.6	10.1±0.9
F150L	4	26.9±3.6	12.3±0.6
F150M	6	56.3±3.2	11.4±0.5
F150N	5	8.1±3.1	12.7±0.7
F150P	6	-7.7±4.2	13.1±0.7
F150Q	8	-6.9±3.4	11.1±0.5
F150R	4	-23.6±5.2	11.6±0.8
F150S	8	29.8±2.5	13.2±0.7
F150T	8	22.9±2.7	15.6±0.8
F150V	6	31.8±3.2	11.1±0.7
F150W	9	5.8±3.2	13.4±0.9
F150Y	5	7.0±3.2	10.7±0.6

$V_{1/2}$ and *k* values were derived from the *Boltzmann* fit and obtained from fitting conductance versus voltage (*G*-*V*) relations. Values shown as mean ± SEM.

Table.S2 The physicochemical properties of amino acids including hydrophobicity and side chain volume. Related to Figure 1.

Amino acid at position 150	*Hydrophobicity (Kyte-Doolittle)*	*Hydrophobicity (Goldman-Engelman-Steitz)*	*Side chain volume ($Å^3$)*
A	1.8	1.6	88.6
C	2.5	2.0	108.5
D	-3.5	-9.2	111.1
E	-3.5	-8.2	138.4
F	2.8	3.7	189.9
G	-0.4	1.0	60.1
H	-3.2	-3.0	153.2
I	4.5	3.1	166.7
K	-3.9	-8.8	168.6
L	3.8	2.8	166.7
M	1.9	3.4	162.9
N	-3.5	-4.8	114.1
P	-1.6	-0.2	112.7
Q	-3.5	-4.1	143.8
R	-4.5	-12.3	173.4
S	-0.8	0.6	89.0
T	-0.7	1.2	116.1
V	4.2	2.6	140.0
W	-0.9	1.9	227.8
Y	-1.3	-0.7	193.6

Table.S3 Effects of mutations in S2 and S4 segments on the voltage-dependent activation of H_v1 channels. Related to Figures 1-2.

Channel	*n*	$V_{1/2}$*(mV)*	*k(mV)*	ΔG_0*(kjmol^{-1})*	$\lvert\Delta\Delta G_0\rvert$*(kjmol^{-1})*
WT	10	61.7±2.7	11.6±0.4	13.1±0.3	*n/a*
R1K	6	117.2±3.4	14.3±1.3	20.8±1.2	*n/a*
R2K	6	25.3±4.0	10.2±1.0	6.1±0.4	*n/a*
R3K	8	96.6±5.1	14.1±1.0	17.2±0.6	*n/a*
N4K	6	52.7±2.3	8.0±0.9	17.1±1.5	*n/a*
F150W	9	5.8±3.2	13.4±0.9	0.8±0.5	*n/a*
F150W-R1K	7	78.9±4.7	17.6±0.9	11.1±0.3	2.7±1.4
F150W-R2K	7	22.1±2.1	14.7±1.1	3.8±0.4	10.1±0.9
F150W-R3K	6	119.2±3.2	17.8±1.2	17.0±1.2	12.1±1.5
F150W-N4K	6	6.8±2.3	8.3±1.0	2.6±1.0	2.2±1.8
D112E	8	43.3±3.6	10.8±0.6	10.3±1.1	*n/a*
D112E-F150W	6	15.8±2.6	10.7±0.7	3.9±0.9	6.0±1.6
D112E-F150W-R2K	6	31.7±0.9	14.0±1.0	5.8±0.6	4.9±1.4
D112E-F150W-R3K	6	125.0±3.0	16.3±1.4	19.8±2.2	5.8±2.6
F149W	6	57.5±2.1	12.3±0.4	11.6±0.6	*n/a*
F149W-R2K	5	18.8±1.5	9.2±0.7	5.1±0.4	0.6±0.9
F149W-R3K	5	98.6±4.9	18.8±1.2	13.1±0.9	2.6±1.3
M151W	6	44.2±3.5	9.7±0.6	11.7±1.5	*n/a*
M151W-R2K	4	54.0±3.1	16.5±0.6	8.1±0.4	3.5±1.6
M151W-R3K	4	83.3±4.3	17.0±0.7	12.2±0.9	3.6±1.8

$V_{1/2}$ and k values were derived from the *Boltzmann* fit and obtained from fitting *G-V* relations. Values shown as mean ± SEM. ΔG_0 and $|\Delta\Delta G_0|$ were determined by the equations shown in the methods. *n/a*, not applicable.

Table S4. List of primers used for mutagenesis. Related to STAR Methods.

Constructs	***Type***	***Primer Sequences (5' to 3')***
F150A	Forward	GAGCATCACCATCTTGGTCTTTGCTATGATGGAGATCATC
	Reverse	GATGATCTCCATCATAGCAAAGACCAAGATGGTGATGCTC
F150C	Forward	GCATCACCATCTTGGTCTTTTGTATGATGGAGATCATC
	Reverse	GATGATCTCCATCATACAAAAGACCAAGATGGTGATGC
F150D	Forward	CATGAGCATCACCATCTTGGTCTTTGATATGATGGAGATCATC
	Reverse	GATGATCTCCATCATATCAAAGACCAAGATGGTGATGCTCATG
F150E	Forward	CATGAGCATCACCATCTTGGTCTTTGAGATGATGGAGATCATC
	Reverse	GATGATCTCCATCATCTCAAAGACCAAGATGGTGATGCTCATG
F150G	Forward	GAGCATCACCATCTTGGTCTTTGGTATGATGGAGATCATC
	Reverse	GATGATCTCCATCATACCAAAGACCAAGATGGTGATGCTC
F150H	Forward	CATGAGCATCACCATCTTGGTCTTTCATATGATGGAGATCATC
	Reverse	GATGATCTCCATCATATGAAAGACCAAGATGGTGATGCTCATG
F150I	Forward	GAGCATCACCATCTTGGTCTTTATTATGATGGAGATCATC
	Reverse	GATGATCTCCATCATAATAAAGACCAAGATGGTGATGCTC
F150K	Forward	CATGAGCATCACCATCTTGGTCTTTAAGATGATGGAGATCATC
	Reverse	GATGATCTCCATCATCTTAAAGACCAAGATGGTGATGCTCATG
F150L	Forward	GCATCACCATCTTGGTCTTTTTGATGATGGAGATCATC
	Reverse	GATGATCTCCATCATCAAAAAGACCAAGATGGTGATGC
F150M	Forward	CATGAGCATCACCATCTTGGTCTTTATGATGATGGAGATCATC
	Reverse	GATGATCTCCATCATCATAAAGACCAAGATGGTGATGCTCATG
F150N	Forward	CATGAGCATCACCATCTTGGTCTTTAATATGATGGAGATCATC
	Reverse	GATGATCTCCATCATATTAAAGACCAAGATGGTGATGCTCATG
F150P	Forward	GAGCATCACCATCTTGGTCTTTCCTATGATGGAGATCATC
	Reverse	GATGATCTCCATCATAGGAAAGACCAAGATGGTGATGCTC
F150Q	Forward	CATGAGCATCACCATCTTGGTCTTTCAGATGATGGAGATCATC
	Reverse	GATGATCTCCATCATCTGAAAGACCAAGATGGTGATGCTCATG
F150R	Forward	CATGAGCATCACCATCTTGGTCTTTAGGATGATGGAGATCATC

	Reverse	GATGATCTCCATCATCCTAAAGACCAAGATGGTGATGCTCATG
F150S	Forward	CATGAGCATCACCATCTTGGTCTTTAGTATGATGGAGATCATC
	Reverse	GATGATCTCCATCATACTAAAGACCAAGATGGTGATGCTCATG
F150T	Forward	CATGAGCATCACCATCTTGGTCTTTACTATGATGGAGATCATC
	Reverse	GATGATCTCCATCATAGTAAAGACCAAGATGGTGATGCTCATG
F150V	Forward	GCATCACCATCTTGGTCTTTGTTATGATGGAGATCATC
	Reverse	GATGATCTCCATCATAACAAAGACCAAGATGGTGATGC
F150W	Forward	GAGCATCACCATCTTGGTCTTTTGGATGATGGAGATCATC
	Reverse	GATGATCTCCATCATCCAAAAGACCAAGATGGTGATGCTC
F150Y	Forward	GAGCATCACCATCTTGGTCTTTTATATGATGGAGATCATC
	Reverse	GATGATCTCCATCATATAAAAGACCAAGATGGTGATGCTC
R1K (R205K)	Forward	CCTGCTGATTCTGCTCAAGCTGTGGCGGGTG
	Reverse	CACCCGCCACAGCTTGAGCAGAATCAGCAGG
R2K (R208K)	Forward	CTCCGGCTGTGGAAGGTGGCCCGGATC
	Reverse	GATCCGGGCCACCTTCCACAGCCGGAG
R3K (R211K)	Forward	GCTGTGGCGGGTGGCCAAGATCATCAATGGG
	Reverse	CCCATTGATGATCTTGGCCACCCGCCACAGC
N4K (N214K)	Forward	GTGGCCCGGATCATCAAAGGGATTATCATCTC
	Reverse	GAGATGATAATCCCTTTGATGATCCGGGCCAC
R3C (R211C)	Forward	CTGTGGCGGGTGGCCTGCATCATCAATGGG
	Reverse	CCCATTGATGATGCAGGCCACCCGCCACAG
D112E	Forward	GGTTCTGGAAGCCCTCCTGGTGCTTGCTG
	Reverse	GAGGGCTTCCAGAACCACCAAGCAGATGATG
F149W	Forward	CTTGGTCTGGTTTATGATGGAGATCATCTTTAAATTATTTG
	Reverse	CCATCATAAACCAGACCAAGATGGTGATGCTCATG
M151W	Forward	CTTTTTTTGGATGGAGATCATCTTTAAATTATTTGTC
	Reverse	GATCTCCATCCAAAAAAAGACCAAGATGGTGATGCTC